

Accepted Manuscript

High levels of eukaryotic Initiation Factor 6 (eIF6) are required for immune system homeostasis and for steering the glycolytic flux of TCR-stimulated CD4⁺ T cells in both mice and humans

Nicola Manfrini, Sara Ricciardi, Annarita Miluzio, Maya Fedeli, Alessandra Scagliola, Simone Gallo, Daniela Brina, Thure Adler, Dirk H. Busch, Valerie Gailus-Durner, Helmut Fuchs, Martin Hrabě de Angelis, Stefano Biffo

PII: S0145-305X(17)30273-2

DOI: [10.1016/j.dci.2017.07.022](https://doi.org/10.1016/j.dci.2017.07.022)

Reference: DCI 2950

To appear in: *Developmental and Comparative Immunology*

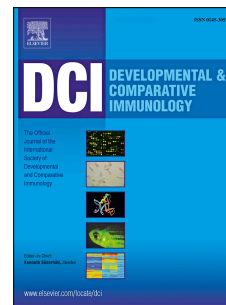
Received Date: 14 May 2017

Revised Date: 21 July 2017

Accepted Date: 21 July 2017

Please cite this article as: Manfrini, N., Ricciardi, S., Miluzio, A., Fedeli, M., Scagliola, A., Gallo, S., Brina, D., Adler, T., Busch, D.H., Gailus-Durner, V., Fuchs, H., Hrabě de Angelis, M., Biffo, S., High levels of eukaryotic Initiation Factor 6 (eIF6) are required for immune system homeostasis and for steering the glycolytic flux of TCR-stimulated CD4⁺ T cells in both mice and humans, *Developmental and Comparative Immunology* (2017), doi: [10.1016/j.dci.2017.07.022](https://doi.org/10.1016/j.dci.2017.07.022).

This is a PDF file of an unedited manuscript that has been accepted for publication. As a service to our customers we are providing this early version of the manuscript. The manuscript will undergo copyediting, typesetting, and review of the resulting proof before it is published in its final form. Please note that during the production process errors may be discovered which could affect the content, and all legal disclaimers that apply to the journal pertain.



1 **High levels of eukaryotic Initiation Factor 6 (eIF6) are required for immune system**
2 **homeostasis and for steering the glycolytic flux of TCR-stimulated CD4⁺ T cells in both mice**
3 **and humans**

4 Nicola Manfrini^{a*+}, Sara Ricciardi^{a+}, Annarita Miluzio^a, Maya Fedeli^b, Alessandra Scagliola^{a,c},
5 Simone Gallo^{a,c}, Daniela Brina^d, Thure Adler^{e§}, Dirk H. Busch^f, Valerie Gailus-Durner^e, Helmut
6 Fuchs^e, Martin Hrabě de Angelis^{e,g,h}, Stefano Biffo^{a,c*}

7

8 ^a National Institute of Molecular Genetics “Romeo ed Enrica Invernizzi” - INGM, via F. Sforza 35,
9 20122 Milan, Italy.

10 ^b Experimental Immunology Unit, Division of Immunology, Transplantation and Infectious
11 Diseases, DIBIT, H. San Raffaele Scientific Institute, via Olgettina 58, 20132 Milan, Italy.

12 ^c Department of Biosciences, University of Milan, Via Celoria 26, 20133 Milan, Italy.

13 ^d Molecular Oncology Group, Institute of Oncology Research (IOR), Oncology Institute of Southern
14 Switzerland (IOSI), Via Mirasole 22A, Bellinzona, Switzerland

15 ^e German Mouse Clinic, Institute of Experimental Genetics, Helmholtz Zentrum München, German
16 Research Center for Environmental Health, 85764 Neuherberg, Germany.

17 ^f Institute for Medical Microbiology, Immunology and Hygiene, Technische Universität München,
18 Trogerstrasse 30, 81675 Munich, Germany.

19 [§] Center of Life and Food Sciences Weihenstephan, Technische Universität München, 85354
20 Freising, Germany.

21 ^h German Center for Diabetes Research, 85764 Neuherberg, Germany.

22

23 § present address: Comprehensive Pneumology Center, Institute of Lung Biology and Disease ,
24 Helmholtz Zentrum München, German Research Center for Environmental Health, 85764
25 Neuherberg, Germany

26

27 * Address correspondence to: Nicola Manfrini: tel. +390200660309; fax. +390200660216;
28 manfrini@ingm.org; Stefano Biffo: tel. +390200660304; fax. +390200660216; biffo@ingm.org

29

30

31 ⁺ The two authors contributed equally to the work

32

33

34

35 Abstract

36 Eukaryotic Initiation Factor 6 (eIF6) is required for 60S ribosomal subunit biogenesis and efficient
37 initiation of translation. Intriguingly, in both mice and humans, endogenous levels of eIF6 are
38 detrimental, as they act as tumor and obesity facilitators, raising the question on the evolutionary
39 pressure that maintains high eIF6 levels. Here we show that in mice and humans, high levels of
40 eIF6 are required for proper immune functions. First, eIF6 heterozygous (het) mice show an
41 increased mortality during viral infection and a reduction of peripheral blood CD4⁺ Effector
42 Memory T cells. In human CD4⁺ T cells, eIF6 levels rapidly increase upon T-cell receptor
43 activation and drive the glycolytic switch and the acquisition of effector functions. Importantly, in
44 CD4⁺ T cells, eIF6 levels control interferon- γ (IFN- γ) secretion without affecting proliferation. In
45 conclusion, the immune system has a high evolutionary pressure for the maintenance of a dynamic
46 and powerful regulation of the translational machinery.

47

48 **Keywords:** eIF6, Immune system, CD4⁺ T cells, effector functions, metabolism, glycolysis.

49 **Abbreviations:** eIF6: eukaryotic Initiation Factor 6; het: heterozygous;
50 IFN- γ : interferon- γ ; TCM: central memory T cell; TEM: effector memory T cell; DN: double
51 negative; DP: double positive; SP: single positive.

52

53 Highlights

54 High levels of eIF6 are required for a proper immune response

55 eIF6 het mice succumb to viral infection

56 Generation of Effector Memory T cells requires high eIF6 activity

57 eIF6 positively regulates the glycolytic activation of CD4⁺ T lymphocytes

58

59

60 1. Introduction

61 mRNA translation is a well-organized process divided into four consequential phases: initiation,
62 elongation, termination and recycling. Initiation is held as the rate limiting step for the translation of
63 most mRNAs (Sonenberg and Hinnebusch, 2009). Eukaryotic initiation factor 6 (eIF6) was
64 originally characterized as a monomeric anti-association ribosomal factor binding 60S ribosomal
65 subunits and blocking 40S subunit recruitment, thus impeding formation of a translationally active
66 80S (Valenzuela et al., 1982). Later studies unequivocally demonstrated that eIF6 is necessary for
67 60S maturation (Sanvito et al., 1999) and is part of the 66S pre-ribosomal particle (Volta et al.,
68 2005). eIF6 release from the 60S during ribosomal maturation can be due to the combined action of
69 Shwachman-Bodian-Diamond Syndrome (SBDS) and Elongation Factor Like GTPase 1 (EFL1)
70 proteins (Finch et al., 2011; Menne et al., 2007).

71 In spite of its nucleolar role, eIF6 is more abundant in the cytoplasm than in the nucleus (Biffo et
72 al., 1997): eIF6 partial depletion in mice leads to a deficit in its cytoplasmic pool, resulting in
73 inefficient translation downstream of insulin and growth factor administration (Gandin et al., 2008).
74 A current model proposes that eIF6 prevents unproductive ribosome joining by clamping free 60S
75 ribosomal subunits and impairing their binding to the non mRNA-loaded 40S ribosomal subunits
76 (Miluzio et al., 2009). eIF6 is phosphorylated and activated by the Receptor for Activated C-Kinase
77 1 (RACK1)/Protein kinase C beta (PKC β) axis (Ceci et al., 2003). Such phosphorylation favours
78 eIF6 removal from the 60S ribosomal subunit and the consequent formation of translationally active
79 80S ribosomes. In mice, RACK1 depletion partly phenocopies eIF6 depletion (Volta et al., 2013),
80 and in fruitfly, RACK1 itself has been shown to control the specific translation of viral IRES
81 regulated mRNAs (Majzoub et al., 2014). Thus, eIF6 and RACK1 may affect translation either
82 alone or by cooperating with one another (Gallo and Manfrini, 2015).

83 The importance of eIF6 is clear in pathological conditions (Miluzio et al., 2016). eIF6 levels have
84 been shown to correlate with insulin resistance and obesity. In fact, eIF6 het mice are protected by
85 diet-induced obesity and lipid steatosis and, in hepatocytes, eIF6 controls lipogenesis and glycolysis
86 through translational regulation of transcriptional factors (Brina et al., 2015b). eIF6 is also
87 important in regulating tumor progression, as its overexpression correlates with poor prognosis in
88 certain human cancers (Miluzio et al., 2015; Sanvito et al., 2000). Evidence for eIF6 gene
89 amplification has been recently presented in human breast cancer (Gatza et al., 2014) and restriction
90 of eIF6 activity dramatically protects from oncogenic-mediated transformation, *in vitro*, and from
91 Myc-induced lymphomagenesis, *in vivo* (Miluzio et al., 2011). It was also shown that eIF6
92 depletion impairs lactate and ATP production in malignant pleural mesothelioma cells, leading to
93 growth reduction (Miluzio et al., 2015). In summary, eIF6 acts as a rate-limiting initiation factor
94 downstream of insulin and growth factors signaling and regulates metabolism in physiological
95 conditions, cancer, and metabolic syndromes. Since eIF6 het mice, which express half the levels of
96 eIF6, are healthier than wild type (wt) littermates, being overall less prone to metabolic syndromes
97 (Brina et al., 2015b) and resistant to oncogenesis (Miluzio et al., 2011), we asked whether there was
98 a physiological pressure for maintaining high levels of eIF6.

99 Recent RNAseq (Bonnal et al., 2015) and proteomic data (Mitchell et al., 2015) revealed that
100 eIF6 is highly expressed in lymphoid cells. What is more, high levels of eIF6 mRNA were detected
101 in T cells within hours of *in vivo* activation (Orr et al., 2012). Thus, we hypothesized that high eIF6
102 levels are required for immune regulation. This consideration together with the observation that
103 eIF6 het mice succumbed to an unwanted viral infection led us to characterize eIF6 role in T
104 lymphocytes. Our results suggest that eIF6 is necessary for overall immune system functionality
105 and in particular for the metabolic switch required for CD4⁺ T cell activation. In this context we can
106 envisage eIF6 as a novel regulator of the immune response and speculate that its functions are
107 exerted as a translational regulator acting upstream of transcription (Brina et al., 2015b) .

108

109

110 2. Materials and methods

111 2.1. Mouse colony

112 eIF6^{+/-} mice were generated as previously described (Gandin et al., 2008) and backcrossed to the
113 C57BL6/N strain for 22 generations, to obtain a pure genetic background. The health status of mice
114 was monitored every month according to the Federation of European Laboratory Animal Science
115 Associations (FELASA) recommendations. Animals were genotyped and randomly analyzed and
116 all experiments were performed on age-matched male mice. Primary cells were derived from
117 thymus and blood of littermates of the specified genotypes.

118 All the experiments involving mice were performed in accordance to Italian national regulations
119 and experimental protocols were reviewed and approved by the local Institutional Animal Care and
120 Use Committees of the San Raffaele Research Institute (IACUC n. 688). At the German Mouse
121 Clinic (GMC), mice were maintained according to the GMC housing conditions and German laws.
122 All tests performed at the GMC were approved by the responsible authority of the Regierung von
123 Oberbayern.

124

125 2.2. Immunology screen, blood samples from mice

126 Blood samples were collected from isoflurane-anesthetized mice (14 weeks old males; 10 wt, 8
127 eIF6 het) by puncturing the retro-bulbar sinus with non-heparinized glass capillaries (1.0 mm in
128 diameter; Neolab; Munich, Germany). Blood was then collected in heparinized tubes (Li-heparin,
129 KABE, Art.No. 078028; Nümbrecht, Germany). Each tube was immediately inverted and then left
130 at RT for two hours. Cells and plasma were then separated by centrifugation (10 minutes, 5000G;
131 8°C). Plasma was collected while the cell pellet was used for FACS analyses. From this pellet,
132 frequencies of the main circulating peripheral blood leukocytes (PBLs) were measured by flow
133 cytometry. PBLs were isolated from the cell pellet of 500 µl whole blood samples. The cell pellet

134 was dissolved in 600 μ l NH_4Cl -based, TRIS-buffered erythrocyte lysis solution, and 150 μ l
135 transferred into 96-well micro titer plates. After washing steps with FACS staining buffer, PBLs
136 were incubated for 20 minutes with Fc block (clone 2.4G2, PharMingen, San Diego, USA). Cells
137 were then stained with fluorescence-conjugated monoclonal antibodies (PharMingen). After
138 incubation propidium iodide was added for the identification of dead cells (Zamai et al., 1996)
139 which might unspecifically bind to antibodies and/or lose specific antigens upon apoptosis (Diaz et
140 al., 2004). Samples were acquired from 96 well plates and measured with a three laser 10-color
141 flow cytometer (LSRII, Becton Dickinson, USA; Gallios, Beckman Coulter, USA). At least 30,000
142 living $\text{CD}45^+$ cells per sample were analyzed. Intact cells were identified by their FSC/SSC profile
143 and dead cells were gated out according to their propidium iodide signal. Living cells were then
144 gated through the SSC/CD45 signal (Weaver et al., 2001). The following stainings were performed
145 to identify the different leukocytes populations:

146 Staining 1) T cells ($\text{CD}3^+$), $\text{CD}4^+$ T cells, $\text{CD}8^+$ T cells (see also Manfrini et al., 2017).

147 Staining 2) on $\text{CD}4^+$ T cells, naïve ($\text{CD}62\text{L}^+ \text{CD}44^-$), Cm ($\text{CD}62\text{L}^+ \text{CD}44^+$) and Em ($\text{CD}62\text{L}^-$
148 $\text{CD}44^+$).

149

150 *2.3. Isolation and activation of human $\text{CD}4^+$ T cells*

151 Blood buffy coat cells of healthy donors were obtained from Fondazione I.R.C.C.S. Ca' Granda
152 Ospedale Maggiore Policlinico, Milan, Italy. Peripheral blood mononuclear cells were isolated by
153 Ficoll-paque density gradient centrifugation. The ethical committee of I.R.C.C.S. Ca' Granda
154 Ospedale Maggiore Policlinico Foundation approved the use of PBMCs from healthy donors for
155 research purposes and all methods and experiments were performed in accordance with the relevant
156 guidelines and regulations. Informed consent was obtained from all subjects. Human blood primary
157 $\text{CD}4^+$ naïve T cells were purified > 95% by negative selection with magnetic beads with the
158 isolation kit for human $\text{CD}4^+$ Naïve T cells (Miltenyi Biotec) followed by cell sorting using the

159 following combination of surface markers: CD4⁺, CD62L⁺, CD45RO⁻. Experiments *in vitro* were
160 performed by activating naïve CD4⁺ T cells with Human T-Activator CD3/CD28 Dynabeads (Life
161 Technologies) and cultured for the indicated time intervals in RPMI medium with 10% FBS, 0.1%
162 Penicillin/Streptomycin (EuroClone), 0.1 % nonessential amino acids (Lonza), and 0,1% Sodium
163 Pyruvate (Lonza) at 37°C and 5% CO₂. IL-2 was added at 20 IU/ml (202-IL; R&D Systems).

164 2.4. Lentiviral production

165 HEK 293T cells were transfected with: packaging plasmid ENV, pMDG, pΔ8.74 and pGIPZ
166 plasmids carrying scramble shRNA or eIF6-specific shRNAs (Open Biosystem). Viral supernatant
167 was collected and titrated 48-72 hours later.

169 2.5. mRNA extraction and real-time RT-PCR

170 Total RNA was extracted from cells with TRIzol reagent (Invitrogen). RNA was then purified
171 with the RNeasy extraction kit (Qiagen). DNA was removed from RNA samples by using the on-
172 column RNase free DNase set (Qiagen). Reverse transcription was performed with the SuperScript
173 III First-Strand kit (Invitrogen) using random hexamers and according to the manufacturer's
174 instructions. Reverse transcribed complementary DNAs (200 ng) were amplified with specific
175 primers. The Taqman probe specific for eIF6 (Mm04208296_m1) was used. Target mRNA
176 quantification was assessed by quantitative reverse-transcriptase realtime PCR (qRT-PCR) using a
177 Taqman Universal PCR Master Mix (cat no. 4324018, Applied Biosystems), with 18S rRNA as an
178 internal standard (Applied Biosystems, cat no. 4333760F). Reactions were performed on a
179 StepOnePlus Real-Time PCR System (Thermo Fisher Scientific). The data are expressed as
180 absolute mRNA levels of the target genes. Results are represented as means +/- standard deviation
181 of three independent experiments.

183 2.6. Western blotting and antibodies

184 SDS-PAGE was performed on protein extracts obtained from human CD4⁺ naïve T cell samples
185 differentiated *in vitro*. See “Isolation and activation of human CD4⁺ T cell” paragraph for details.
186 Samples were homogenized in RIPA buffer (10 mM Tris-HCl, pH 7.4, 1% sodium deoxycholate,
187 1% Triton X-100, 0.1% SDS, 150 mM NaCl and 1 mM EDTA, pH 8.0). The following antibodies
188 were used: mouse monoclonal antibody against eIF6 (1:3000) (Biffo et al., 1997) and β -actin
189 (1:10,000; AC-15) A5441 Sigma. Chemiluminescent signals were detected using Amersham ECL
190 Prime (GE Healthcare Life Sciences) and images were acquired using the LAS-3000 imaging
191 system from Fuji. eIF6 protein levels were quantified by densitometric analysis using ImageJ and
192 were normalized to β -actin abundance.

193

194 2.7. Measurement of lactate secretion

195 Cell culture supernatants of naïve and *in vitro* activated CD4⁺ T cells infected with the Scr-sh or
196 eIF6-sh constructs were collected. Lactate secreted into the medium was measured using the Lactate
197 Assay Kit (Biovision) following manufacturer’s instructions. The average fluorescent intensities
198 were calculated for replicates of each condition. Values were normalized to protein contents
199 obtained from the same wells (Duvel et al., 2010).

200

201 2.8. ATP content analysis

202 CD4⁺ naïve and 4 days-activated T cells previously infected with the Scr-sh or eIF6-sh constructs
203 were homogenized in 6% (v/v) ice-cold HClO₄. Extracts were then centrifuged at 10,000g for
204 10 min at 4 °C. The acid supernatant was neutralized with K₂CO₃ and used for luminometric
205 determination of ATP (ATP determination kit, Molecular Probes) using the method of Lundin
206 (Lopez-Lluch et al., 2006) as modified in (Calamita et al., 2017).

207

208 2.9. Measurement of IFN- γ production

209 Cell culture supernatants of naïve and *in vitro* activated CD4⁺ T cells infected with the Scr-sh or
210 eIF6-sh constructs were collected and analyzed for IFN- γ content using the DuoSet ELISA
211 development system for human IFN- γ detection (R&D Systems cat no. DY285). Samples were
212 prepared according to the manufacturer's instructions. IFN- γ levels for each sample were
213 normalized to total protein content.

214

215 2.10. Proliferation assay

216 Proliferation was assessed by CellTrace-CFSE (ThermoFisher Scientific) staining of 5×10^4
217 FACS-purified CD4⁺ naïve T cells isolated from the blood of three healthy donors. Cells were
218 grown in RPMI media with 10% FBS, 0.1% Penicillin/Streptomycin (EuroClone), 0.1 %
219 nonessential amino acids (Lonza), and 0.1% Sodium Pyruvate (Lonza) at 37°C and 5% CO₂ and
220 activated with Human T-Activator CD3/CD28 Dynabeads (Life Technologies) and IL-2 20 IU/ml
221 (202-IL; R&D Systems) for five days. At day 5 post-activation cells were FACS-analyzed for CFSE
222 content. Naïve unstimulated cells were also stained and analyzed as a control.

223

224 2.11. Statistical analysis

225 All the results were analyzed with the two-tailed *t*-test. A *p*-value of <0.05 was considered
226 significant (**p* < 0.05; ***p* < 0.01; ****p* < 0.001; NS: not significant). Kaplan-Meier curve was
227 validated by the Log-rank (Mantel-Cox) test.

228

229

230 3. Results

231 3.1. eIF6 het mice show a reduction of peripheral CD4⁺ T cells and succumb to infections

232 In physiological conditions eIF6 het mice are phenotypically normal, resistant to diet-induced
233 obesity and less susceptible to Myc-induced lymphomagenesis compared to wt littermates (Brina et

234 al., 2015a; Miluzio et al., 2011). eIF6 het mice have half eIF6 protein levels compared to wt animals
235 and reduced insulin- and growth factor-stimulated translation (Gandin et al., 2008). Preliminary
236 studies on humoral antibody response did not show gross differences between eIF6 wt and het mice.
237 This notion was revived by the observation that an unwanted mouse norovirus (MNV) infection in
238 the animal house claimed victims only in the eIF6 het population and not in the wt. Quantification
239 of the affected subcolonies indeed confirmed that eIF6 het mice had higher mortality compared to
240 wt controls (Fig. 1A). Death was accompanied by wasting and diarrhea. Next, we quantified
241 immune cells in the peripheral blood of wt and eIF6 het mice (Fig. 1B and Fig. 1 in Manfrini et al.,
242 2017). We did not see significant differences in the number of total leukocytes in peripheral blood
243 ($9.86 \times 10^3/\text{mm}^3$ for wt eIF6 mice vs $8.72 \times 10^3/\text{mm}^3$ for het eIF6 mice; p -value: 0.083) and no
244 significant differences in the frequencies of granulocytes, monocytes and B cells (see Fig. 1A and
245 1B, left in Manfrini et al., 2017). Although we did not see any significant difference in the
246 proportions of CD3^+ T cells in the blood (see Fig. 1B, right in Manfrini et al., 2017), by subdividing
247 the CD3^+ T cell compartment into CD4^+ or CD8^+ subpopulations, we found a significant lower
248 frequency of CD4^+ T cells in het mice compared to controls (p -value: 0.04) (Fig. 1B, left), but no
249 significant difference in the proportions of CD8^+ T cells (p -value: 0.39) (Fig. 1B, right). This
250 apparent discrepancy can be explained by the simple fact that CD4^+ T cells are a subgroup of the
251 more vast CD3^+ T cell repertoire and that relevant differences occurring in the abundance of the
252 CD4^+ T cell subset are not necessarily able to cause significant alterations in overall CD3^+ T cell
253 abundance. Taken together these data indicate that under baseline conditions eIF6 levels are rate
254 limiting for T cell homeostasis.

255 The reduction in CD4^+ positive T cells in eIF6 het mice coupled to the increased mortality upon
256 infection suggest that the generation of specific effector cells could be impaired. We therefore
257 analyzed if there were significant alterations in the proportions of CD4^+ naïve, central memory
258 (TCM) and effector memory (TEM) T cells subpopulation in the blood of wt and eIF6 het mice
259 (Fig. 2A). In line with the expectations, the percentages of naïve and TCM cells were not altered in

260 eIF6 het mice compared to controls (Fig.2A, left and center histograms). In contrast, the TEM
261 subpopulation showed a drastic decrease (Fig. 2A, right histogram).

262 We asked whether differences in the T cell repertoire were only observed in the peripheral blood
263 or also evident in the thymus where T cells develop through positive and negative selection.
264 Precursor cells enter the thymus as double negative (DN) $CD4^-CD8^-$ thymocytes but then
265 upregulate both CD4 and CD8 co-receptor molecules to become $CD4^+CD8^+$ double positive (DP)
266 thymocytes. DP thymocytes develop into $CD4^+$ or $CD8^+$ lineages as single positive (SP) T cells
267 (Luckheeram et al., 2012). Therefore, we sought to determine whether the observed reduction of
268 $CD4^+$ T cells in the blood of eIF6 het mice might have been the result of impaired $CD4^+$ T cell
269 selection in the thymus (Weinreich and Hogquist, 2008). To test this possibility, we analyzed
270 thymocyte populations in eIF6 het mice and in control animals taking advantage of the fact that
271 different stages of thymocyte maturation can be easily followed by the expression of different
272 surface markers (Germain, 2002). Among the DN population we found no significant differences
273 neither in the proportions of $CD44^+ CD25^-$ early T lineage progenitors cells, nor in that of $CD44^+$
274 $CD25^+$, $CD44^- CD25^+$ and $CD44^- CD25^-$ cell populations (see Fig. 2A in Manfrini et al., 2017). The
275 overall proportions of thymic DN ($CD4^- CD8^-$), DP ($CD4^+ CD8^+$) and SP ($CD4^+ CD8^-$, $CD4^- CD8^+$)
276 cells also remained unchanged between eIF6 het and wt animals (see Fig. 2B in Manfrini et al.,
277 2017). These data raise the point that the reduced percentage of peripheral blood $CD4^+$ T cells in
278 eIF6 het mice cannot be ascribed to defective $CD4^+$ T cell selection in the thymus.

279 In summary, in mice haploinsufficient for eIF6, increased mortality upon infection is accompanied
280 by a reduced number of TEM cells in the periphery, leading us to ask whether also in humans eIF6
281 played a role in peripheral lymphocyte activation and polarization.

282

283 *3.2. In human $CD4^+$ T cells eIF6 expression is triggered by TCR stimulation*

284 At first, we interrogated a human lymphocyte RNAseq dataset for eIF6 expression levels in *ex vivo*
285 isolated naïve, TCM and TEM cell subpopulations (Bonnal et al., 2015). Both TCM and TEM cells
286 showed increased levels of eIF6 compared to resting naïve T cells (Fig. 3A), suggesting that eIF6
287 might have an important role in preserving the peripheral T cell milieu also in humans.

288 *In vivo*, commitment and thus full activation of a CD4⁺ naïve T cell requires CD3 activation and
289 co-stimulation of the CD28 receptor (Seo and Taniuchi, 2016). Similarly *in vitro*, human naïve
290 CD4⁺ T cells can be easily fully activated and stimulated to proliferate, using magnetic beads
291 conjugated with anti-CD3/CD28 monoclonal antibodies (mAbs) and interleukin 2 (IL-2) (Trickett
292 and Kwan, 2003). We isolated peripheral blood mononuclear cells (PBMCs) from blood of healthy
293 donors and performed a detailed analysis of eIF6 expression both at the RNA and protein levels in
294 naïve CD4⁺ T cells left untreated or activated *in vitro* for 1, 2 or 3 days with anti-CD3/CD28 beads
295 and IL-2 (Fig. 3B). We found that eIF6 mRNA levels drastically peak after 1 day of activation and
296 tend to slowly decrease towards baseline levels at the third day of culture (Fig. 3C). Untreated CD4⁺
297 naïve T cells featured a modest but detectable amount of eIF6 protein (Fig. 3D). eIF6 protein levels
298 increased after 1 day of T-cell receptor (TCR) activation and the accumulation continued over the
299 entire time course of the experiment (Fig. 3D). Taken together, these results show that, upon T cell
300 activation, eIF6 expression is induced both at the mRNA and protein levels and suggest a role for
301 eIF6 during CD4⁺ T cell activation.

302

303 *3.3. eIF6 downregulation in human CD4⁺ T cells affects proper acquisition of effector functions*
304 *and impairs TCR-dependent stimulation of glycolysis*

305 Upon activation, CD4⁺ naïve T cells undergo a precise and fast metabolic reprogramming,
306 including a rapid activation of aerobic glycolysis (Chang et al., 2013). In mice hepatocytes and
307 human mesothelioma eIF6 upregulation drives a glycolytic switch (Brina et al., 2015b; Miluzio et
308 al., 2015). We investigated whether eIF6 may be pivotal in orienting metabolic fluxes also in human

309 lymphocytes. We analyzed the glycolytic and energy production capacity of human CD4⁺ T cells
310 activated *in vitro* for 4 days and transduced with lentiviral vectors expressing either a constitutive
311 eIF6 shRNA (eIF6-sh) or a scramble control (Scr-sh) (Fig. 4A). We confirmed eIF6 downregulation
312 both at the RNA and protein level at day 4 post-activation (Fig. 4B-C). Our analysis revealed that
313 glycolysis was significantly decreased in activated CD4⁺ T cells depleted for eIF6 compared to
314 control cells, as determined by a reduction in lactate secretion. (Fig. 4D). Consistent with decreased
315 glycolysis, CD4⁺ T cells depleted for eIF6 displayed a decreased energy production capacity
316 compared to controls, as indicated by a drastic reduction of ATP levels (Fig. 4E).

317 Next, we explored, *in vitro*, the consequences of eIF6 depletion on the acquisition of effector
318 functions by activated CD4⁺ T cells. After activation, following an initial growth phase, naïve
319 CD4⁺ T cells rapidly divide, acquire effector functions and start producing inflammatory cytokines,
320 among which IFN- γ (Van der Pouw-Kraan et al., 1992). Therefore we analyzed cytokine secretion
321 and found that eIF6-depleted CD4⁺ T cells produced less IFN- γ compared to control cells (Fig.
322 4F). In some cell types, eIF6 downmodulation can cause a reduced G1/S phase progression and
323 impaired proliferation (Miluzio et al., 2015; Ricciardi et al., 2015). To exclude the possibility that
324 the effects of eIF6 depletion on acquisition of effector functions in T cells were an indirect
325 outcome of defective proliferation, we evaluated the percentage of cells entering the cell cycle by
326 carboxyfluorescein succinimidyl ester (CFSE) analysis. After 5 days of induction the percentage of
327 dividing cells was comparable between Scr-sh and eIF6-sh samples (Fig. 4G), indicating that, as
328 previously reported, eIF6 depletion does not affect the cell cycle entry of activated CD4⁺ T cells
329 (Orr et al., 2012).

330

331 4. Discussion

332 In this study we unequivocally demonstrate that high levels of eIF6 are required for proper
333 immunological functions. The fact that eIF6 het mice succumb to infections reconciles with the
334 paradox that, in the lab, eIF6 het mice are more fit than wt littermates. Indeed, eIF6 het mice are

335 resistant to B cell lymphomas (Miluzio et al., 2011) and to insulin resistance upon a high fat diet
336 (Brina et al., 2015b). We conclude that the evolutionary pressure for high eIF6 levels may be
337 particularly strong in the CD4⁺ T lineage. This finding will be discussed in the context of the
338 relevance of translational control in immune cells.

339 Primary human T cells are also highly sensitive to eIF6 depletion. In spite of the relatively low
340 downregulation of eIF6 by shRNAs, which may be due either to technical issues such as incomplete
341 lentiviral infection of primary human cells, or to the fact that the high transcriptional activity of the
342 eIF6 gene during activation supplies a steady-state level of translated mRNA, we observe reduced
343 glycolysis, ATP depletion and reduced cytokine production. These observations confirm the general
344 model by which translational activity of eIF6 is particularly relevant in the regulation of metabolism
345 (Brina et al., 2015b). Given that, on one side eIF6 het mice are much more susceptible to MNV
346 infection than wt littermates, and on the other, activated CD4⁺ T cells depleted for eIF6 show
347 defective inflammatory cytokine secretion, it is tempting to hypothesize that high eIF6 levels are
348 essential for both innate and adaptive immune system response to viral infection. Moreover,
349 considering that the T_h1 differentiation program strongly depends on IFN- γ (Lighvani et al., 2001;
350 Zhu et al., 2010) and that T_h1 CD4⁺ T cells act as helper cells for the antiviral and cytotoxic activity
351 of CD8⁺ T cells, eIF6 could act as a regulator of T_h1-dependent immune responses. In general,
352 however eIF6 levels seem particularly relevant in the glycolytic switch observed in the effector
353 response.

354 The mechanistic role of translation in the immune response is far from being understood in spite
355 of the evidence of its importance (Piccirillo et al., 2014). Initiation is the rate limiting step of
356 translation (Loreni et al., 2014; Sonenberg and Hinnebusch, 2009) and mounting evidence indicates
357 that targeting the translational machinery is feasible and leads to specific effects (Bhat et al., 2015).
358 Specifically, triggering initiation of translation by positive signals such as growth factors and
359 cytokines can be regulated through sequential activation of the 48S complex by eIF4F formation,
360 followed by the release of eIF6 from the 60S subunit and the formation of an active 80S ribosome

361 (Loreni et al., 2014). Importantly, 48S activation strongly depends on mTORC1 that, through the
362 phosphorylation of 4E-BPs, releases the cap-binding protein eIF4E allowing it to be recruited into
363 the eIF4F complex (Sonenberg and Hinnebusch, 2009). Genetic evidence in mice demonstrates that
364 4E-BPs levels completely control the sensitivity to mTORC1 inhibition (Dowling et al., 2010).
365 Indeed T lymphocytes contain high levels of the 4E-BP2 isoform which regulates rapamycin-
366 sensitive growth and proliferation (So et al., 2016). The effect of rapamycin on T cells is
367 pleiotropic, but it consistently induces a transition towards an immunosuppressive phenotype,
368 accompanied by a reduction of glycolysis (Maciolek et al., 2014). In summary, mTOR activation
369 leads to a robust translationally-driven program that is essential for full differentiation of effector
370 cells thanks to a strong translational and metabolic activation. In this context, our data on eIF6 are
371 intriguing and exciting because they demonstrate that also activation of eIF6, which is not directly
372 dependent on mTOR, is rate limiting for switching the metabolism of T cells and for a complete
373 immunological response. Since eIF6 is activated downstream of the Ras-PCK pathway and
374 functions by allowing 60S recruitment and 80S formation, events which mechanistically follow 48S
375 formation (Miluzio et al., 2016), we conclude that full activation of an immune response requires
376 the simultaneous activation of both the mTOR and Ras-PKC cascades which are independent and
377 rate limiting.

378 Next, it will be important to define the specific mRNAs whose translation is strongly dependent
379 on eIF6 activity. The use of novel technologies such as ribosome profiling will be pivotal to define
380 which mRNAs are essential in T cell activation.

381

382

383 **Conflict of Interest Disclosure**

384 The authors declare no commercial or financial conflict of interest.

385

386 Acknowledgments, author contributions and funding

387 We thank Moira Paroni for her useful help with preliminary ELISAs.

388 S.B., N.M. and S. R. conceived the project. N.M. and S. R. contributed equally to the work by
389 designing, analyzing and performing most of the experiments. A. M., M. F., A. S., and T.A.
390 performed experiments and analyzed the data. D.H.B., H.F., V.G-D. M.HdA. participated in the
391 conception of the immunology phenotyping of mice. S.G. helped interpreting the data. N.M. wrote
392 the manuscript. S. B., S.G. and S.R. edited the manuscript draft. All the authors provided critical
393 revision of the manuscript.

394 Studies were funded by the European Research Council (ERC) under grant “Translate” n. 338999 to
395 S.B. and by the German Federal Ministry of Education and Research to the GMC (Infrafrontier
396 grant 01KX1012).

397

398

399 References

- 400 Bhat, M., Robichaud, N., Hulea, L., Sonenberg, N., Pelletier, J., Topisirovic, I., 2015. Targeting the translation
401 machinery in cancer. *Nat Rev Drug Discov* 14, 261-278.
- 402 Biffo, S., Sanvito, F., Costa, S., Preve, L., Pignatelli, R., Spinardi, L., Marchisio, P.C., 1997. Isolation of a novel
403 beta4 integrin-binding protein (p27(BBP)) highly expressed in epithelial cells. *J Biol Chem* 272, 30314-
404 30321.
- 405 Bonnal, R.J., Ranzani, V., Arrigoni, A., Curti, S., Panzeri, I., Gruarin, P., Abrignani, S., Rossetti, G., Pagani, M.,
406 2015. De novo transcriptome profiling of highly purified human lymphocytes primary cells. *Sci Data* 2,
407 150051.
- 408 Brina, D., Miluzio, A., Ricciardi, S., Biffo, S., 2015a. eIF6 anti-association activity is required for ribosome
409 biogenesis, translational control and tumor progression. *Biochim Biophys Acta* 1849, 830-835.
- 410 Brina, D., Miluzio, A., Ricciardi, S., Clarke, K., Davidsen, P.K., Viero, G., Tebaldi, T., Offenhauser, N., Rozman,
411 J., Rathkolb, B., Neschen, S., Klingenspor, M., Wolf, E., Gailus-Durner, V., Fuchs, H., Hrabe de Angelis, M.,
412 Quattrone, A., Falciani, F., Biffo, S., 2015b. eIF6 coordinates insulin sensitivity and lipid metabolism by
413 coupling translation to transcription. *Nat Commun* 6, 8261.
- 414 Calamita, P., Miluzio, A., Russo, A., Pesce, E., Ricciardi, S., Khanim, F., Cheroni, C., Alfieri, R., Mancino, M.,
415 Gorrini, C., Rossetti, G., Peluso, I., Pagani, M., Medina, D.L., Rommens, J., Biffo, S., 2017. SBDS-Deficient
416 Cells Have an Altered Homeostatic Equilibrium due to Translational Inefficiency Which Explains their
417 Reduced Fitness and Provides a Logical Framework for Intervention. *PLoS Genet* 13, e1006552.
- 418 Ceci, M., Gaviraghi, C., Gorrini, C., Sala, L.A., Offenhauser, N., Marchisio, P.C., Biffo, S., 2003. Release of eIF6
419 (p27BBP) from the 60S subunit allows 80S ribosome assembly. *Nature* 426, 579-584.
- 420 Chang, C.H., Curtis, J.D., Maggi, L.B., Jr., Faubert, B., Villarino, A.V., O'Sullivan, D., Huang, S.C., van der
421 Windt, G.J., Blagih, J., Qiu, J., Weber, J.D., Pearce, E.J., Jones, R.G., Pearce, E.L., 2013. Posttranscriptional
422 control of T cell effector function by aerobic glycolysis. *Cell* 153, 1239-1251.

- 423 Diaz, D., Prieto, A., Barcenilla, H., Monserrat, J., Prieto, P., Sánchez, M.A., Reyes, E., Hernandez-Fuentes,
424 M.P., de la Hera, A., Orfao, A., Alvarez-Mon, M., 2004. Loss of lineage antigens is a common feature of
425 apoptotic lymphocytes. *Journal of leukocyte biology* 76, 609-615.
- 426 Dowling, R.J., Topisirovic, I., Alain, T., Bidinosti, M., Fonseca, B.D., Petroulakis, E., Wang, X., Larsson, O.,
427 Selvaraj, A., Liu, Y., Kozma, S.C., Thomas, G., Sonenberg, N., 2010. mTORC1-mediated cell proliferation, but
428 not cell growth, controlled by the 4E-BPs. *Science* 328, 1172-1176.
- 429 Duvel, K., Yecies, J.L., Menon, S., Raman, P., Lipovsky, A.I., Souza, A.L., Triantafellow, E., Ma, Q., Gorski, R.,
430 Cleaver, S., Vander Heiden, M.G., MacKeigan, J.P., Finan, P.M., Clish, C.B., Murphy, L.O., Manning, B.D.,
431 2010. Activation of a metabolic gene regulatory network downstream of mTOR complex 1. *Molecular cell*
432 39, 171-183.
- 433 Finch, A.J., Hilcenko, C., Basse, N., Drynan, L.F., Goyenechea, B., Menne, T.F., Gonzalez Fernandez, A.,
434 Simpson, P., D'Santos, C.S., Arends, M.J., Donadieu, J., Bellanne-Chantelot, C., Costanzo, M., Boone, C.,
435 McKenzie, A.N., Freund, S.M., Warren, A.J., 2011. Uncoupling of GTP hydrolysis from eIF6 release on the
436 ribosome causes Shwachman-Diamond syndrome. *Genes Dev* 25, 917-929.
- 437 Gallo, S., Manfrini, N., 2015. Working hard at the nexus between cell signaling and the ribosomal
438 machinery: An insight into the roles of RACK1 in translational regulation. *Translation (Austin)* 3, e1120382.
- 439 Gandin, V., Miluzio, A., Barbieri, A.M., Beugnet, A., Kiyokawa, H., Marchisio, P.C., Biffo, S., 2008. Eukaryotic
440 initiation factor 6 is rate-limiting in translation, growth and transformation. *Nature* 455, 684-688.
- 441 Gatzka, M.L., Silva, G.O., Parker, J.S., Fan, C., Perou, C.M., 2014. An integrated genomics approach identifies
442 drivers of proliferation in luminal-subtype human breast cancer. *Nature genetics* 46, 1051-1059.
- 443 Germain, R.N., 2002. T-cell development and the CD4-CD8 lineage decision. *Nat Rev Immunol* 2, 309-322.
- 444 Lighvani, A.A., Frucht, D.M., Jankovic, D., Yamane, H., Aliberti, J., Hissong, B.D., Nguyen, B.V., Gadina, M.,
445 Sher, A., Paul, W.E., O'Shea, J.J., 2001. T-bet is rapidly induced by interferon-gamma in lymphoid and
446 myeloid cells. *Proceedings of the National Academy of Sciences of the United States of America* 98, 15137-
447 15142.
- 448 Lopez-Lluch, G., Hunt, N., Jones, B., Zhu, M., Jamieson, H., Hilmer, S., Cascajo, M.V., Allard, J., Ingram, D.K.,
449 Navas, P., de Cabo, R., 2006. Calorie restriction induces mitochondrial biogenesis and bioenergetic
450 efficiency. *Proc Natl Acad Sci U S A* 103, 1768-1773.
- 451 Loreni, F., Mancino, M., Biffo, S., 2014. Translation factors and ribosomal proteins control tumor onset and
452 progression: how? *Oncogene* 33, 2145-2156.
- 453 Luckheeram, R.V., Zhou, R., Verma, A.D., Xia, B., 2012. CD4(+)T cells: differentiation and functions. *Clin Dev*
454 *Immunol* 2012, 925135.
- 455 Maciolek, J.A., Pasternak, J.A., Wilson, H.L., 2014. Metabolism of activated T lymphocytes. *Curr Opin*
456 *Immunol* 27, 60-74.
- 457 Majzoub, K., Hafirassou, M.L., Meignin, C., Goto, A., Marzi, S., Fedorova, A., Verdier, Y., Vinh, J., Hoffmann,
458 J.A., Martin, F., Baumert, T.F., Schuster, C., Imler, J.L., 2014. RACK1 controls IRES-mediated translation of
459 viruses. *Cell* 159, 1086-1095.
- 460 Manfrini, N., Ricciardi, S., Miluzio, A., Fedeli M., Scagliola, A., Gallo, S., Adler, T., Busch, D.H., Gailus-Durner,
461 V., Fuchs, H., Hrabě de Angelis, M., Biffo, S., 2017. Data on the effects of eIF6 downmodulation on the
462 proportions of innate and adoptive immune system cell subpopulations and on thymocyte maturation.
463 Data in Brief, submitted.
- 464 Menne, T.F., Goyenechea, B., Sanchez-Puig, N., Wong, C.C., Tonkin, L.M., Ancliff, P.J., Brost, R.L., Costanzo,
465 M., Boone, C., Warren, A.J., 2007. The Shwachman-Bodian-Diamond syndrome protein mediates
466 translational activation of ribosomes in yeast. *Nat Genet* 39, 486-495.
- 467 Miluzio, A., Beugnet, A., Grosso, S., Brina, D., Mancino, M., Campaner, S., Amati, B., de Marco, A., Biffo, S.,
468 2011. Impairment of cytoplasmic eIF6 activity restricts lymphomagenesis and tumor progression without
469 affecting normal growth. *Cancer Cell* 19, 765-775.
- 470 Miluzio, A., Beugnet, A., Volta, V., Biffo, S., 2009. Eukaryotic initiation factor 6 mediates a continuum
471 between 60S ribosome biogenesis and translation. *EMBO Rep* 10, 459-465.
- 472 Miluzio, A., Oliveto, S., Pesce, E., Mutti, L., Murer, B., Grosso, S., Ricciardi, S., Brina, D., Biffo, S., 2015.
473 Expression and activity of eIF6 trigger malignant pleural mesothelioma growth in vivo. *Oncotarget* 6, 37471-
474 37485.

- 475 Miluzio, A., Ricciardi, S., Manfrini, N., Alfieri, R., Oliveto, S., Brina, D., Biffo, S., 2016. Translational control by
476 mTOR-independent routes: how eIF6 organizes metabolism. *Biochem Soc Trans* 44, 1667-1673.
- 477 Mitchell, C.J., Getnet, D., Kim, M.S., Manda, S.S., Kumar, P., Huang, T.C., Pinto, S.M., Nirujogi, R.S., Iwasaki,
478 M., Shaw, P.G., Wu, X., Zhong, J., Chaerkady, R., Marimuthu, A., Muthusamy, B., Sahasrabudde, N.A., Raju,
479 R., Bowman, C., Danilova, L., Cutler, J., Kelkar, D.S., Drake, C.G., Prasad, T.S., Marchionni, L., Murakami,
480 P.N., Scott, A.F., Shi, L., Thierry-Mieg, J., Thierry-Mieg, D., Irizarry, R., Cope, L., Ishihama, Y., Wang, C.,
481 Gowda, H., Pandey, A., 2015. A multi-omic analysis of human naive CD4+ T cells. *BMC Syst Biol* 9, 75.
- 482 Orr, S.J., Boutz, D.R., Wang, R., Chronis, C., Lea, N.C., Thayaparan, T., Hamilton, E., Milewicz, H., Blanc, E.,
483 Mufti, G.J., Marcotte, E.M., Thomas, N.S., 2012. Proteomic and protein interaction network analysis of
484 human T lymphocytes during cell-cycle entry. *Molecular systems biology* 8, 573.
- 485 Piccirillo, C.A., Bjur, E., Topisirovic, I., Sonenberg, N., Larsson, O., 2014. Translational control of immune
486 responses: from transcripts to translomes. *Nat Immunol* 15, 503-511.
- 487 Ricciardi, S., Miluzio, A., Brina, D., Clarke, K., Bonomo, M., Aiolfi, R., Guidotti, L.G., Falciani, F., Biffo, S.,
488 2015. Eukaryotic translation initiation factor 6 is a novel regulator of reactive oxygen species-dependent
489 megakaryocyte maturation. *J Thromb Haemost* 13, 2108-2118.
- 490 Sanvito, F., Piatti, S., Villa, A., Bossi, M., Lucchini, G., Marchisio, P.C., Biffo, S., 1999. The beta4 integrin
491 interactor p27(BBP/eIF6) is an essential nuclear matrix protein involved in 60S ribosomal subunit assembly.
492 *J Cell Biol* 144, 823-837.
- 493 Sanvito, F., Vivoli, F., Gambini, S., Santambrogio, G., Catena, M., Viale, E., Veglia, F., Donadini, A., Biffo, S.,
494 Marchisio, P.C., 2000. Expression of a highly conserved protein, p27BBP, during the progression of human
495 colorectal cancer. *Cancer research* 60, 510-516.
- 496 Seo, W., Taniuchi, I., 2016. Transcriptional regulation of early T-cell development in the thymus. *Eur J*
497 *Immunol* 46, 531-538.
- 498 So, L., Lee, J., Palafox, M., Mallya, S., Woxland, C.G., Arguello, M., Truitt, M.L., Sonenberg, N., Ruggero, D.,
499 Fruman, D.A., 2016. The 4E-BP-eIF4E axis promotes rapamycin-sensitive growth and proliferation in
500 lymphocytes. *Sci Signal* 9, ra57.
- 501 Sonenberg, N., Hinnebusch, A.G., 2009. Regulation of translation initiation in eukaryotes: mechanisms and
502 biological targets. *Cell* 136, 731-745.
- 503 Trickett, A., Kwan, Y.L., 2003. T cell stimulation and expansion using anti-CD3/CD28 beads. *J Immunol*
504 *Methods* 275, 251-255.
- 505 Valenzuela, D.M., Chaudhuri, A., Maitra, U., 1982. Eukaryotic ribosomal subunit anti-association activity of
506 calf liver is contained in a single polypeptide chain protein of Mr = 25,500 (eukaryotic initiation factor 6). *J*
507 *Biol Chem* 257, 7712-7719.
- 508 Van der Pouw-Kraan, T., Van Kooten, C., Rensink, I., Aarden, L., 1992. Interleukin (IL)-4 production by
509 human T cells: differential regulation of IL-4 vs. IL-2 production. *Eur J Immunol* 22, 1237-1241.
- 510 Volta, V., Beugnet, A., Gallo, S., Magri, L., Brina, D., Pesce, E., Calamita, P., Sanvito, F., Biffo, S., 2013. RACK1
511 depletion in a mouse model causes lethality, pigmentation deficits and reduction in protein synthesis
512 efficiency. *Cellular and molecular life sciences : CMLS* 70, 1439-1450.
- 513 Volta, V., Ceci, M., Emery, B., Bachi, A., Petfalski, E., Tollervey, D., Linder, P., Marchisio, P.C., Piatti, S., Biffo,
514 S., 2005. Sen34p depletion blocks tRNA splicing in vivo and delays rRNA processing. *Biochem Biophys Res*
515 *Commun* 337, 89-94.
- 516 Weaver, J.L., Broud, D.D., McKinnon, K., Germolec, D.R., 2001. Serial phenotypic analysis of mouse
517 peripheral blood leukocytes. *Toxicology Mechanisms and Methods* 12, 95-118.
- 518 Weinreich, M.A., Hogquist, K.A., 2008. Thymic emigration: when and how T cells leave home. *J Immunol*
519 181, 2265-2270.
- 520 Zamai, L.L., Falcieri, E.E., Marhefka, G.G., Vitale, M.M., 1996. Supravital exposure to propidium iodide
521 identifies apoptotic cells in the absence of nucleosomal DNA fragmentation. *Cytometry Part A* 23, 303-311.
- 522 Zhu, J., Yamane, H., Paul, W.E., 2010. Differentiation of effector CD4 T cell populations (*). *Annu Rev*
523 *Immunol* 28, 445-489.

524

525 **Figure Legends**

526 **Figure 1.** eIF6 het mice show higher mortality upon spontaneous Norovirus infection and decreased
527 levels of peripheral CD4⁺ T cells compared to control animals.

528 (A) Kaplan-Meier curve of eIF6^{+/-} mice (n = 100) compared to eIF6^{+/+} animals (n = 100).

529 Kaplan-Meier curve was validated by the Log-rank (Mantel-Cox) test (*p*-value : 0.0003).

530 (B) Among the living CD3⁺ T cell subpopulation of samples described in Fig.1B of Manfrini et al.,
531 2017, proportions of CD4⁺ and CD8⁺ T cells were assessed.

532 Error bars represent Standard Deviation. Statistical *p*-values were calculated using the two-tailed *t*-
533 test (NS: *p*-value > 0.05; *: *p*-value < 0.05; CD4⁺ T cell % *p*-value: 0.04; CD8⁺ T cell % *p*-value:
534 0.39).

535

536 **Figure 2.** eIF6 het mice have a decreased level of peripheral TEM cells compared to control
537 animals.

538 (A) Proportions of naïve, TCM and TEM cells were assessed among the CD4⁺ T cell population
539 described in Fig. 1B. Representative gating strategies are shown (left).

540 Error bars represent Standard Deviation. Statistical *p*-values were calculated using the two-tailed *t*-
541 test (NS: *p*-value > 0.05; ***: *p*-value < 0.001; naïve T cells % *p*-value: 0.211; TCM cells % *p*-
542 value: 0.222; TEM cells % *p*-value: 0.0002).

543

544 **Figure 3.** eIF6 expression is induced upon activation of human CD4⁺ T cells.

545 (A) RNAseq data regarding eIF6 levels among naïve, TCM and TEM cell subpopulations. eIF6
546 levels are represented as mean PFKM values (n=5).

547 (B) Naïve CD4⁺ T cells were purified from the peripheral blood of healthy donors. Cells were then
548 activated for 3 days *in vitro* with anti-CD3/CD28 beads and 20U/ml IL-2. Samples were collected
549 every day to assess eIF6 expression by RT-qPCR and western blot.

550 (C) RT-qPCR for eIF6 was performed on samples described in (B). mRNA levels are normalized to
551 18S rRNA abundance and are relative to the expression at d0.

552 (D) Whole cell lysates from samples described in (B) were separated by SDS-page and analyzed by
553 western blotting using anti-eIF6 and anti- β -actin antibodies. Error bars represent Standard
554 Deviation and statistical p -values were calculated using the two-tailed t -test (**: p -value <0.01;
555 ***: p -value < 0.001; TCM p -value: 0.0062; TEM p -value: 0.0034; d1 p -value: 0.0002; d2 p -value:
556 0.00014; d3 p -value: 0.00044). Data for (C) and (D) are representative of three independent
557 experiments ($n = 3$).

558

559 **Figure 4.** In human CD4⁺ T cells, shRNA knockdown of eIF6 dramatically reduces glycolysis and
560 inflammatory cytokine secretion.

561 (A) Human naïve CD4⁺ T cells, isolated from blood of healthy donors, were infected with
562 lentiviruses expressing a scramble shRNA (Scr-sh) or an shRNA against eIF6 (eIF6-sh) and
563 activated *in vitro* for 4 days. Samples were collected at the times indicated to assess lactate, ATP
564 and IFN- γ levels.

565 (B) eIF6 mRNA levels were analyzed by RT-qPCR at the times indicated. mRNA levels are
566 normalized to 18S rRNA abundance and are relative to the expression in the Scr-sh control.

567 (C) Whole cell lysates from samples described in (A) were separated by SDS-page and analyzed by
568 western blotting using anti-eIF6 and anti- β -actin antibodies. The representative gel shown was
569 cropped as indicated by the dividing lines. Protein abundance of eIF6 was quantified and data are
570 presented as ratios over the levels of eIF6 in the Scr-sh control.

571 (D) The level of secreted lactate was detected by fluorescence assays.

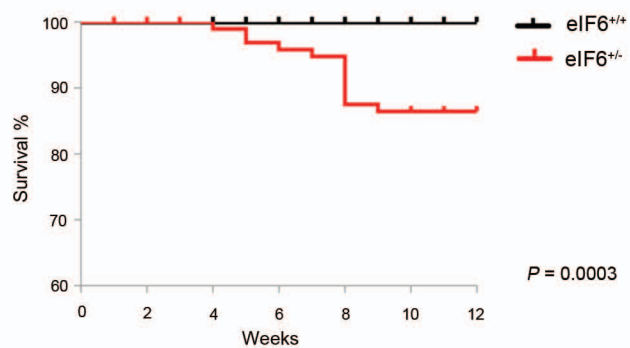
572 (E) ATP levels were detected by luminometric assays and (F) IFN- γ levels were detected by
573 fluorescence assays performed on the samples indicated.

574 (G) Proliferation was assessed using CFSE and monitored after 5 days of *in vitro* anti-CD3/CD28
575 stimulation. Representative plots for day 5 post-stimulation are shown (left). In the CFSE profiles
576 the fitted gaussians, required to determine the rounds of division, are shown in red. Actual CFSE

577 signals are plotted in black. Histograms (right) represent the mean percentage of proliferating Scr-
578 sh and eIF6-sh cells. Error bars represent Standard Deviation, statistical p -values were calculated
579 using the two-tailed t -test (NS: p -value > 0.05 ; *: p -value < 0.05 ; **: p -value < 0.01 ; ***: p -
580 value < 0.001 ; (B) p -value: 0.032; (C) p -value: 0.01; (D) p -value: 0.017; (E) p -value: 0.01; (F) p -
581 value: 0.00026; (G) p -value: 0.63). Data are representative of three independent experiments ($n =$
582 3).

Figure 1

A



B

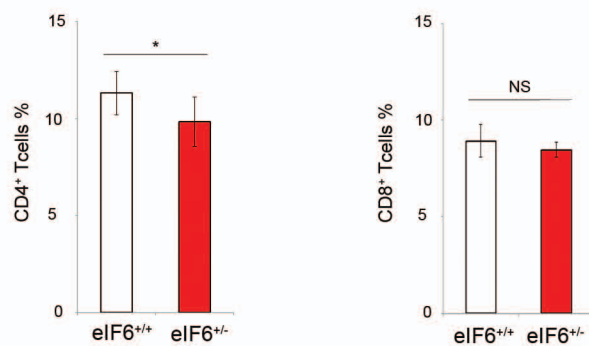


Figure 2

A

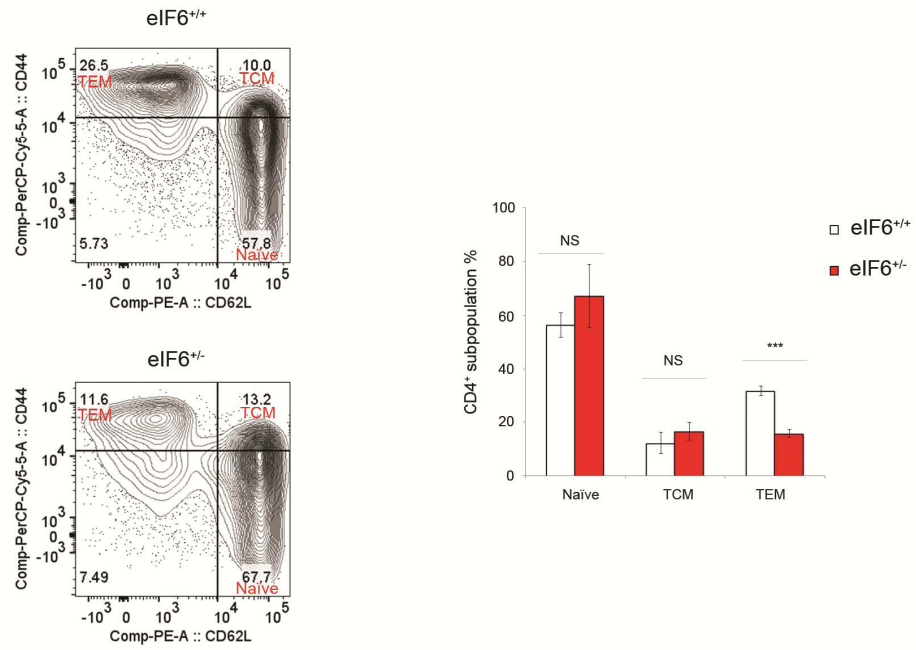


Figure 3

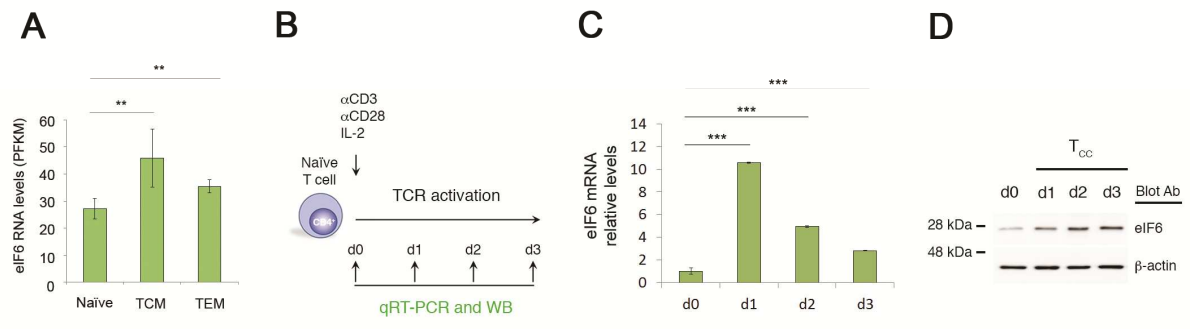
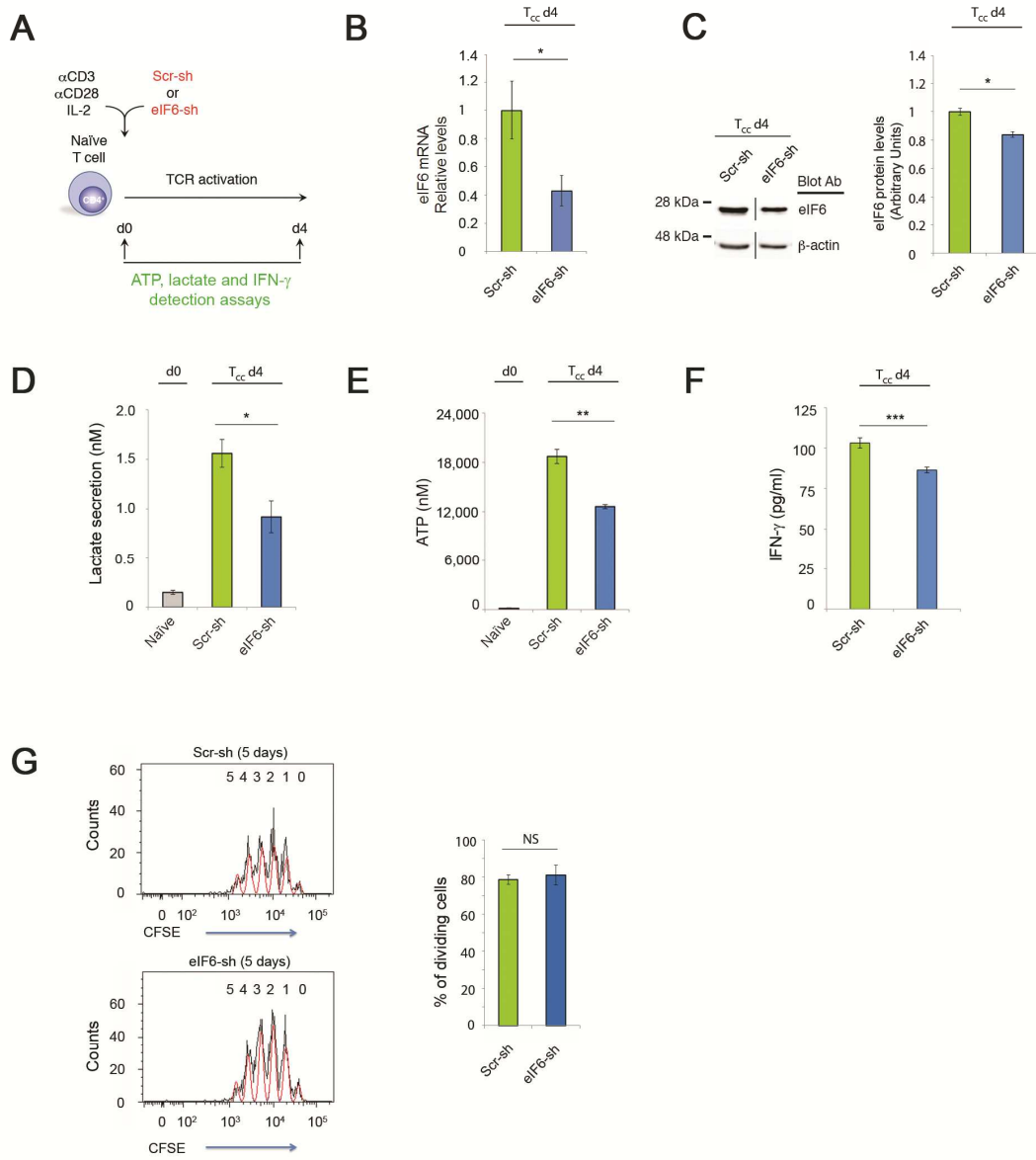


Figure 4



High levels of eukaryotic Initiation Factor 6 (eIF6) are required for immune system homeostasis and for steering the glycolytic flux of TCR-stimulated CD4⁺ T cells in both mice and humans

Highlights

High levels of eIF6 are required for a proper immune response

eIF6 het mice succumb to viral infection

Generation of Effector Memory T cells requires high eIF6 activity

eIF6 positively regulates the glycolytic activation of CD4⁺ T lymphocytes